Heliyon 10 (2024) e26646

Contents lists available at ScienceDirect

Heliyon

journal homepage: www.cell.com/heliyon

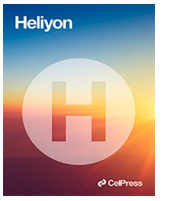

Research article

Cross enclosed square split ring resonator based on D.N.G. metamaterial absorber for X-band glucose sensing application

Muhammad Amir Khalil [a], Wong Hin Yong [a,**], Md Shabiul Islam [a], Ahasanul Hoque [b,*], Cham Chin leei [a], Mohamed S. Soliman [c,d], Mohammad Tariqul Islam [e,***]

[a] Faculty of Engineering (FOE), Multimedia University (MMU), 63100 Cyberjaya, Selangor, Malaysia
[b] Institute of Climate Change, Universiti Kebangsaan Malaysia, Bangi 43600, Selangor, Malaysia
[c] Department of Electrical Engineering, College of Engineering, Taif University, P.O. Box 11099, Taif, 21944, Saudi Arabia
[d] Department of Electrical Engineering, Faculty of Energy Engineering, Aswan University, Aswan 81528, Egypt
[e] Department of Electrical, Electronic and Systems Engineering, Faculty of Engineering and Built Environment, Universiti Kebangsaan Malaysia, Bangi 43600, Selangor, Malaysia

ARTICLE INFO

Keywords:
Sensor
Metamaterial
Glucose
Diabetes

ABSTRACT

This article presents a novel real-time meta-material (MM) sensor based on a non-invasive method that operates in microwave frequency ranges at 8.524 GHz to measure blood glucose levels with quality factor 184 is designed and fabricated. A cross enclosed between two square shapes produces a strong interaction between glucose samples and electromagnetic waves. In this study, 5 were tested noninvasively using the proposed glucose resonant sensor with a range of glucose-level changes from 50 to 130 mg/dL. For this range of glucose-level changes, the frequency detection resolution is 5.06 MHz/(mg/dL), respectively. Despite simulations, fabrication procedures (F.P.) have been carried out for more precise result verification. For the purpose of qualitative analysis, the proposed MM sensor is considered a viable candidate for determining glucose levels.

1. Introduction

Heart rates, blood pressure, and other body metrics can be monitored to ensure a healthy life, and early detection of diseases can be achieved through regular checkups. In recent years, diabetes has become an increasingly deadly disease, and the world can no longer ignore the rise of the disease. A metabolic disorder such as diabetes occurs when the body's glucose levels are out of balance. In 2017, the International Diabetes Federation (I.D.F.) estimated that 451 million adults worldwide had diabetes. If effective prevention methods are not adopted, this number is expected to increase to 693 million by 2045 [1]. Undoubtedly, diabetes mellitus (D.M.) is one of the most prevalent chronic diseases in the world and poor nutrition is a major contributing factor. People with diabetes tend to

* Corresponding author
** Corresponding author.
*** Corresponding author
E-mail addresses: 1211406090@student.mmu.edu.my (M.A. Khalil), hywong@mmu.edu.my (W.H. Yong), shabiul.islam@mmu.edu.my (M.S. Islam), ahasanul@ukm.edu.my (A. Hoque), clcham@mmu.edu.my (C. Chin leei), soliman@tu.edu.sa (M.S. Soliman), tariqul@ukm.edu.my (M. Tariqul Islam).

https://doi.org/10.1016/j.heliyon.2024.e26646
Received 4 May 2023; Received in revised form 26 November 2023; Accepted 16 February 2024
Available online 17 February 2024

experience numerous health problems within their bodies as well as painful treatments for those conditions. In addition, patients with diabetes often suffer from issues with different physical organs or diseases due inability to maintain discipline in their daily life routine, including coronary artery blockages, peripheral arterial, and cerebrovascular (C.V.As.) disease [2].

Furthermore, patients develop skin problems as well as gradually lose their hair. It may become necessary to undergo dialysis at a certain point due to the deterioration of kidney function in the body. Consequently, infections, organ failures, etc., spread over time, and patients often succumb to them and die quickly. In recent years, non-invasive blood glucose (B.G.) monitoring has gained much attention regardless of the currently available invasive techniques [3]. Painless diabetic treatment has become an essential requirement of today's society [4]. Non-invasive glucose measurement can be performed by various advanced electromagnetic (E.M.) wave-based technologies, including infrared spectroscopy, photoacoustic spectroscopy, Raman spectroscopy, fluorescence, optical coherence tomography (OCT), Terahertz spectroscopy, and microwave sensing [5].

A new approach for non-invasive B.G. measurements is now required to make treatment more comfortable and to measure B.G. levels more precisely. Recently, many companies and researchers worldwide have been working toward non-invasive measurements of B.G [6,7]. The finger model has been used in some studies [8]. There is a significant effect on the sensor's frequency response due to the placement of the sample (fingertip). In Ref. [9] presents a design involving a patch reflector and a dielectric resonator (D.R.), which has the appearance of a human thumb. One of the most prominent methods of monitoring B.G. levels is the use of E.M. waves [10]. It is based on the premise that the permittivity (ε) of blood or muscle tissues changes as a function of changes in B.G. levels. Besides EM sensors, different techniques are also available, such as optical spectroscopy or electrochemical sensors. However, the method based on E.M. waves has its advantages with regard to design, ease of use, robustness, fabrication, and cost efficiency [11].

The idea of E.M. wave sensing, primarily at microwave frequencies, was discussed in Ref. [12]. Using tissue-mimicking phantoms, the researchers purported a patch resonator that simultaneously measures B.G. levels and dielectric properties (K). In this work [13,14], sensors were developed to measure glucose concentrations efficiently. In addition, the researchers proposed using a water-glucose solution (W.G.S.) and sampled blood serum to develop highly sensitive sensors. In the past years, research groups [15–17] have been enthusiastically involved in searching for suitable methodologies and developing a microwave and millimetre wave glucose sensing system. The research group has proposed a method for measuring B.G. levels in the human body by using the transmission method at mm-wave frequencies. A simple patch resonator was used, which did not achieve sufficient sensitivity but attained good detection limits. A major focus of reference [18] was the development of the sensors, with measurements being proof of concept rather than actual measurements of diabetes patients or using W.G.S. instead of B.G. solutions. Researchers are investigating the mechanisms by which glucose affects the E.M. field in a patient's blood to develop a non-invasive method for measuring B.G. In the case of microwaving, tissue can be penetrated to a depth of several millimetres or more, depending on the experiment's needs [19]. Another study conducted in Ref. [20] also showed that a milli-meter wave frequency measurement of B.G. levels in the human body could be a useful tool to assess blood sugar levels accurately. However, the technique is being refined to improve its efficiency. This study measures scattering parameters with a Vector Network Analyzer (VNA.) IN5227AU. To simulate scattering parameters, the C.S.T. software program is used. The results of the simulation and the experimental studies were in good agreement. In light of the findings of this study, the cross-enclosed square slit ring resonator is capable of measuring glucose in water and blood accurately and efficiently.

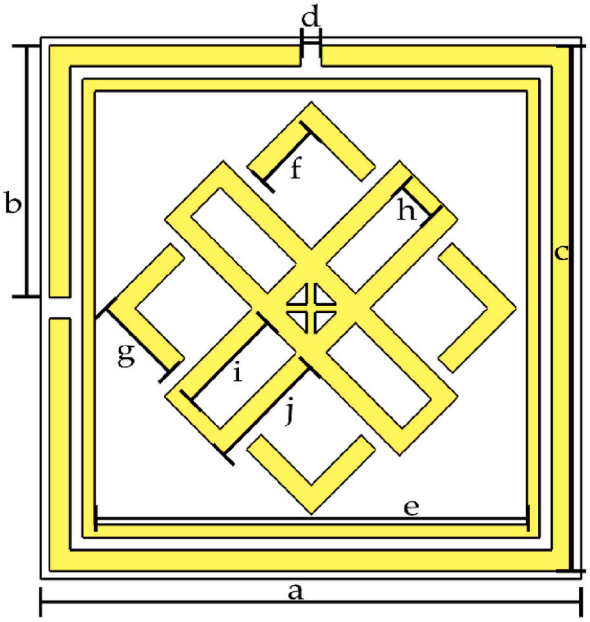

Fig. 1. Schematic of proposed glucose sensor design.

2. Methodology of design and fabrication

The purported non-invasive glucose sensor comprises split ring resonators enclosed closed loop; the geometry is depicted in Fig. 1. The sensor was designed and numerically investigated by Computer Simulation Technology (C.S.T.) studio suite 2022. The overall dimension of the sensor design is $13 \times 13mm$. The sensor is designed on a thin Rogers RT 5880 substrate of height $1.575mm$ and a patch layer that is copper with a thickness of $0.035mm$. The details of the geometrical dimensions are displayed in Table 1. This work proposes a MM biosensor consisting of a cross-shaped patch crammed between square strips. Also, nozzle patches connecting the rectangular sensing area with a radius of 0.20 mm are used. Sensing takes place in a simple cavity within the dielectric substrate. Besides containing the sample, it also produces a capacitance that is proportional to the amount of glucose present. Permeability and permittivity are two crucial factors controlling the electromagnetic response of a material. The intrinsic properties of a material are unique to each material due to its unique composition and atomic configurations [20,21]. MM structures have properties that differ from their constituent materials, where the unit cells behave like electric dipoles [22].

A MM structure exhibits both negative permittivity and permeability at the same time, which is called left-handed metamaterial [23,24]. The mechanism behind the operation of sensors inspired by metamaterials is based on the change in scattering characteristics reflection (S11) and transmission (S21); variations in the permittivity (ε), permeability (μ), or refractive index (η) of the MM based resonator result in a change in the sensed parameters (dielectric change). Since the inductance (L) and capacitance (C) formed for patching depend on lumped components for the microstrip transmission line model, the unit cell sensor was first built using the microstrip transmission line model. Broadband hybrid microcircuits work particularly well with lumped elements where low cost, smaller size and q factors are essential [22]. The recommended design was developed in response to these concerns, according to the study in Ref. [25], along with a comprehensive mathematical model that considers factors such as proximity effects, fringing fields, ground planes, parasites, etc. Microstrip patch optimization and formulation were influenced by wavelength and operating frequency when considering lumped elements of the design followed in Ref. [26]. Further, these components exhibit distinct characteristics, including low Q-factor values and resonance frequencies for S-parameters. The transmission model and our design are illustrated in Fig. 1, in which two rectangles enclose a cross shape with higher Q and inductance. Hence, a numerical calculation will be conducted to determine the equivalent capacitance and inductance, as suggested in reference [25].

$$L(n\mathrm{H}) = 1.25 \times 10^{-3} a \left[In\left(\frac{a+b}{w+t}\right) + 0.078 \right] \mathrm{K}_g \tag{1}$$

Where the value of K_g *and* $C(pF)$ can be determined by Ref. [25].

$$K_g = 0.57 - 0.145 In \frac{\omega_s}{h} \tag{2}$$

$$C(pF) = \frac{10^{-3} \varepsilon_{rd} \omega l}{36 \pi d} \tag{3}$$

Where,

a = Length of the major axis.
b = Length of the minor axis.
l = Micro strip line length.
ω = Micro strip line width.
t = Micro Stip line thickness.
ε_{rd} = Dielectric Constant.
d = Distance between mutual straplines.
ω_s = Width of Substrate.
$h^{'}$ = Thickness of Substrate.

A circuit's capacitance and inductance can be calculated using equations (1) and (3), respectively. Simulation of the proposed design is conducted using Computer Simulation Technology (C.S.T.) 2022, a commercially available software package. A description of the dimensions of the major element is provided in table No. 1.

Table 1
Geometrical dimensions of the proposed structure.

Parameters	Value (mm)	Parameters	Value (mm)
a	13	f	1.70
c	12.60	g	2.20
b	6.05	H	1
d	0.50	I	2.60
e	10.40	J	3

3. Discussion and analysis of the results

3.1. E-field, H-field and surface current analysis

Over the last 150 years, electromagnetic waves have been extensively studied. The wave nature of light was not understood until Maxwell's equations were developed, although the properties of light have been studied since Ancient Greece [27]. A complete description of how the electromagnetic field interacts with the medium can be found in Maxwell's equations [25]:

$$\nabla \times \mathrm{E} = -\frac{\partial B}{\partial t} \tag{4}$$

$$\nabla \times \mathrm{H} = J + \frac{\partial D}{\partial t} \tag{5}$$

$$\nabla \cdot \mathrm{E} = \rho \tag{6}$$

$$\nabla \cdot \mathrm{H} = 0 \tag{7}$$

For electric and magnetic fields, equations (4)–(6) represent Faraday's Law of Induction, Ampere-Maxwell's Law, and Gauss's Law, respectively. Quantities H and E represent magnetic and electric field intensities. They are measured in units of a volt per meter (V/m) and amper per meter (A/m). B and D are known as magnetic induction and electric displacement. A relationship exists between electric and magnetic flux densities as well as electric and magnetic field intensities, referred to as constitutive relations. It is determined by the material in which the field exists and what form it will take. Combining equations (4) and (5) constitutive relations means the Helmholtz equation is obtained [25].

$$\nabla^2 \mathrm{E} = \mu\varepsilon \frac{\partial^2 \mathrm{E}}{\partial t^2} \tag{8}$$

Further, when only the x-component of the electric field is considered, the Helmholtz equation can be derived. Where wave number in the medium can be represented by Ref. [27] $k = \omega\sqrt{\mu\varepsilon}$.

$$\frac{\partial^2 \mathrm{E}_x}{\partial z^2} = \omega^2 \mu\varepsilon \mathrm{E}_x \tag{9}$$

For sinusoidal waves [27],

$$\nabla^2 \mathrm{E} = \mu\sigma j\omega \mathrm{E} + \mu\varepsilon j^2 \omega^2 \mathrm{E} = \gamma^2 \mathrm{E} \tag{10}$$

Helmholtz's equation indicates that electric and magnetic fields are affected by the properties of the medium, such as permittivity, permeability, and wave number. The equations from (4) to (10) are summarized in Refs. [10,25,26]. Consequently, for a resonance frequency of 8.524 GHz, a strong electric field is created by capacitance, as indicated by equation (10) derived from Helmholtz's equation, since the above parameters are nonlinearly related to the propagation constant. There is a similar solution for the distribution of H-fields at resonance frequencies. The homogeneous solution of the field equation distributes the energy of the components of a magnetic field since they are mutually coupled. The H-field and EM-field distributions at resonance frequency are depicted in Fig. 2 (a,b).

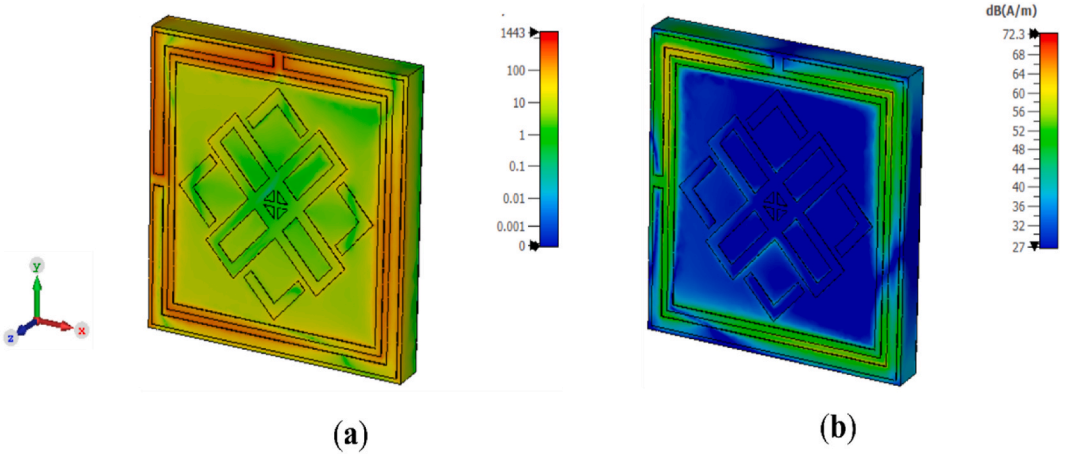

Fig. 2. E M.- field (**a**), H- field (**b**) at resonance frequency at 8.524 (GHz).

Fig. 3 surface current distributions exhibit a significant distribution with high density that is observed as a resonance frequency. Fig. 3 surface current distributions exhibit a significant distribution with high density that is observed as a resonance frequency at 8.524 GHz. Therefore, a travelling wave may encounter a situation where, at low frequency, the wave has a suitable conductor medium. Still, with increasing frequency, the dielectric property of the same medium declines. The dielectric constant can be determined electrostatically by examining the electric dipole moment created by an electron in the presence of a static electric field [10].

$$e\mathrm{E} = m\omega_0^2 \mathrm{X} \tag{11}$$

Equations (12) and (13) can represent the dipole moment per unit volume [10].

$$P = NZ\mathrm{P}_{mol} \equiv \varepsilon_0 \chi_e \mathrm{E} \tag{12}$$

$$\varepsilon = 1 + \frac{NZe^2}{m\omega_0^2 \varepsilon_0} \tag{13}$$

This result appears to change when the dielectric constant exhibits a frequency dependence or when there is a time dependence on the electric field. It is also worth noting that squares, rectangles, at 135° and the central point of the unit cell has a significantly larger surface current area than other parts of the unit cell. This results in a higher concentration of current due to a combination of conduction and displacement currents. There is an intriguing observation that one can observe at the nozzle point. This is where the sensing layer is located. This observation shows that a significant amount of charge elements are travelling back and forth. This could result in a change in capacitance at a central location in the sensing area during sample injection so as to identify the parametric changes for glucose sensing in the suggested design.

3.2. Transmission and reflection performance

The metamaterial biosensor's basic transmission and reflection coefficients were analyzed in C.S.T. microwave studio using the finite integration technique (F.I.T.). Upon the completion of the design, waveguide ports 1 and 2 were subjected to a boundary condition in which no restrictions were imposed on the polarization angle. In order to achieve optimal simulation results, normal conditions of material properties in terms of permittivity, permeability, temperature, and electrical properties were maintained for all simulations. In the unit cell boundary condition, there was an electric field along the X-axis, and a magnetic field along the Y-axis, with the Z-axis left open for field propagation. E.M. field interactions within the targeted frequency range are identified based on this design sensor's reflection coefficient (S11) and transmission coefficient (S21). The reflection and transmission coefficient value at resonance frequency 8.524 GHz, respectively, is −24.24 and −12.37. The reflection and transmission in terms of real and imaginary are depicted in Fig. 4(a and b).

As depicted in Fig. 5 (permittivity and permeability) show the sensor's essential characteristics and Fig. 6 depicated absorption capacity in a simulated environment are illustrated. Reflectance and transmission characteristics were employed to retrieve all of the information. To clarify the characteristics of metamaterial-based sensors, it is necessary to point out that conventional microring resonators are less sensitive than D.N.G. metamaterials since these materials amplify evanescent waves. Furthermore, using such metamaterials has enhanced the system's Sensitivity. Table 2 shows the unit cell's double negative (D.N.G.) values at the resonance frequency. A look at the D.N.G. characteristic of this proposed design, along with the amount of surface current in the sensing layer region at the resonance frequency, will indicate the sensing potentiality of this design and varaiantion in permittivtity show shift in reasonace frequecny.

However, numerical calculations described in Ref. [26] may be used to demonstrate the absorption capabilities of the proposed

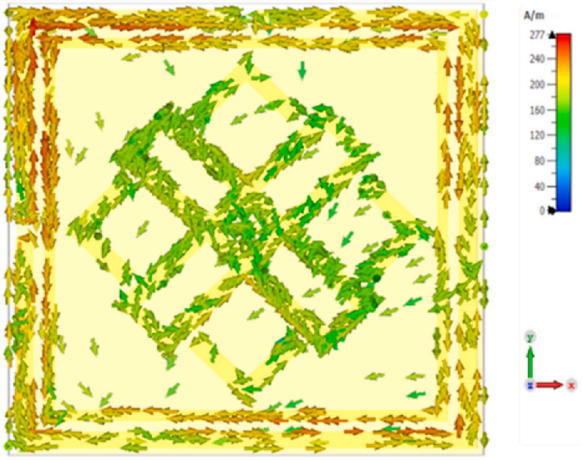

Fig. 3. Surface current distribution at 8.524 GHz.

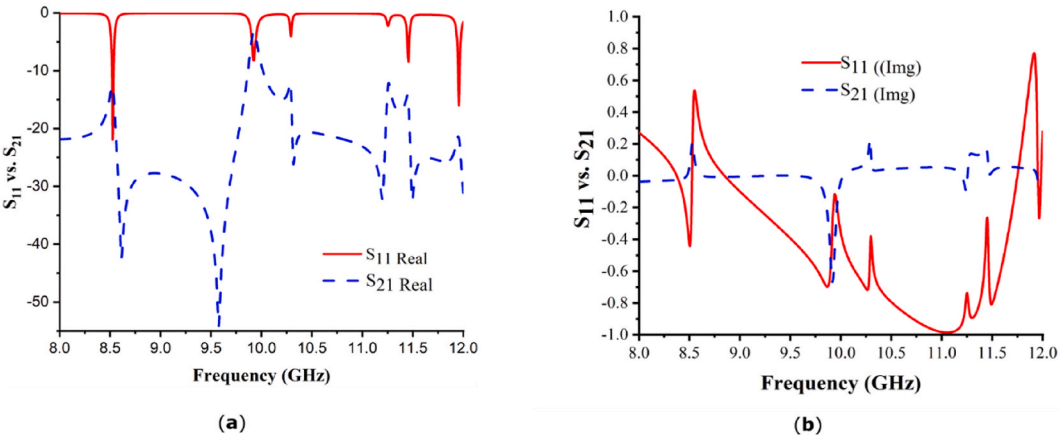

Fig. 4. Reflection and transmission properties (**a**) real (**b**) imaginary.

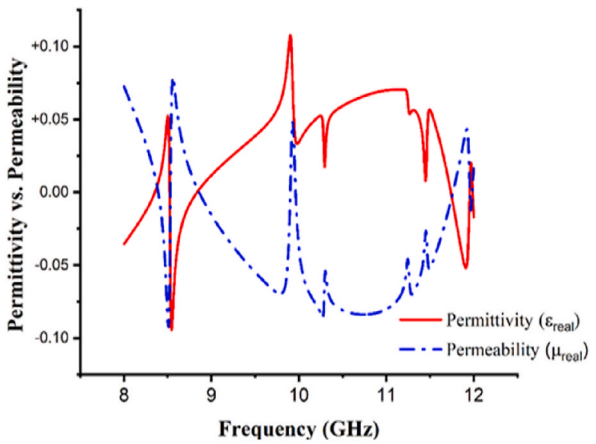

Fig. 5. Simulation performance of the sensor in terms of permittivity and permeability.

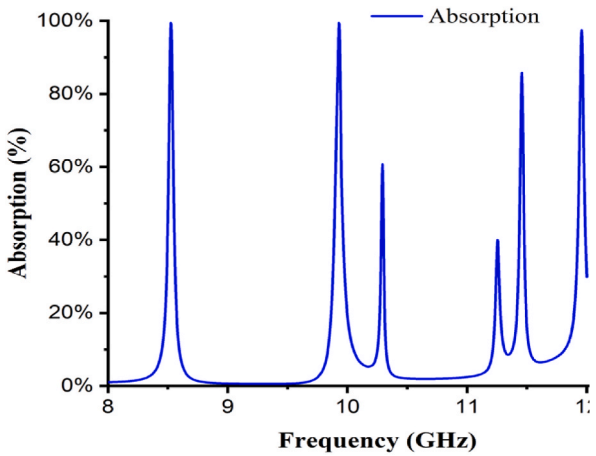

Fig. 6. Absorption with focused frequency spectrum.

Table 2
Double negative values at the resonance frequency.

Resonance Frequency (GHz)	Permittivity ε	Permeability μ	Reflectio Co-efficient η
8.524	−0.095	−0.092	0.0312
11.75	−0.0043	−0.0043	0.0036

structure. It is, therefore, possible to write absorption in the following manner [36]:

$$A = e^{-\alpha d} \tag{14}$$

Where α is the absorption coefficient at a resonance frequency [36]. So,

$$\alpha = \frac{4\pi}{\lambda} K \tag{15}$$

Where K is called the extension coefficient and is equal to $K = \sqrt{\varepsilon_{im}}$.

Based on simulations, we found that the metamaterial-inspired design sensor has suitable properties; by varying the permittivity of the sensing layer between 50 and 90, we can check its sensing capability. Consequently, we can assume that glucose is represented in the water layer and that the difference in distribution means the split gap remains unchanged. An illustration of simulation performance is provided in the following Fig. 7 2-D view and Fig. 8 3-D view.

As can be seen from the graph, there is a significant shift in the reflection parameter when the permittivity of the sensing layer is changed from 50 to 90. On average, there is a shift of 0.037 GHz per step. In order to better understand this, an enlarged image has been included. A further study was conducted on split gap variation to obtain a parametric change for this type of performance. The response of the reflection parameter is depicted in Fig. 9 by changing the split gap from 1 to 1.5 mm. As the split gap increases, it is evident that there is a gradual decrease in shifting value, which shows that a direct impact of mutual capacitance variation on performance can be observed. In order to resolve such resonance

frequency shifting behaviour, P.L.L., which stands for Phase Locked Loop, can be used. The P.L.L. method of deploying wearable sensors would impose a size factor on the development of a device in the case of fluid detection or bio-sensing sensors. Therefore, more comprehensive bandwidth operation is needed when applying bio-sensing, where P.L.L.s might not perform well [22]. A metamaterial-inspired glucose sensor can be used as an alternative to conventional glucose sensors by enhancing the sensor's precision sensing ability. In Table 3, it is shown that the properties of this metamaterial-inspired glucose sensor have been compared to those of a generalized view of their properties that has been used in the past.

3.3. Experimental setups for verification of sensitivity

An experimental setup has been designed to validate the theoretical results, as shown in the figure, while a simulation setup is depicted in Fig. 10. In Fig. 11 (a), the complete simulation step is depicted. While Fig. 11 (b) represents a transparent view of the simulation step. At the crosse shape centre, we placed a glucose sample and measured it reflection coefficient. The experimental setup

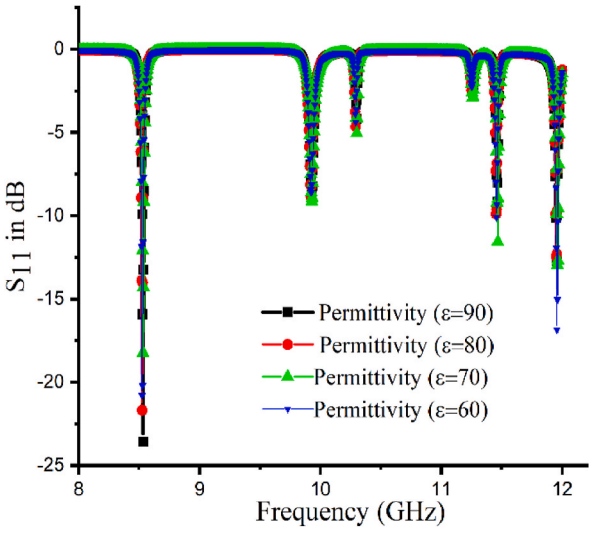

Fig. 7. Reflection Coefficient simulation regarding dielectric constant (**2-D view**).

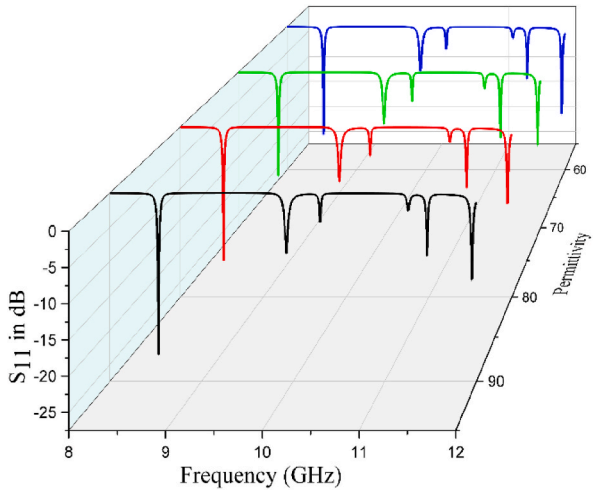

Fig. 8. Reflection Coefficient simulation regarding dielectric constant (**3-D view**).

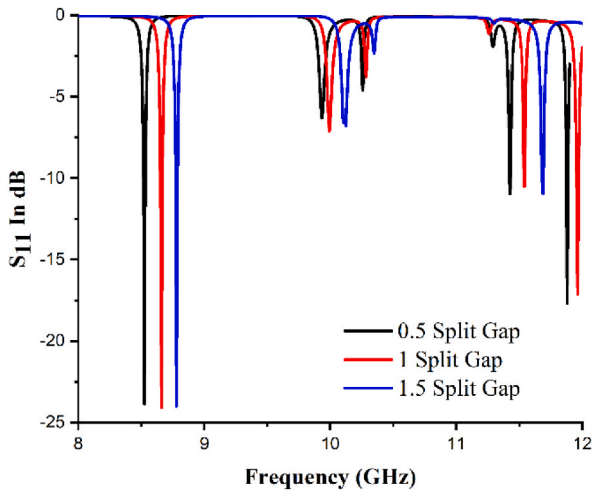

Fig. 9. Responce of reflection parameter by changing split gap.

consists of an IN5227AU Vector Network Analyzer, a fabricated unit cell model, coaxial cable, and a sensing area with a glucose sample. Fig. 12 decipted simulated and measured result for the reflection cofficient for glucose sample at 50 mg/dL.

This study obtained five samples aqueous solution, ranging in glucose concentration from 40 to 130 mg/dL. One drop of serum was poured at a time onto the sensing area using an injection needle, with each drop containing approximately 30 mg/dL. The sensing area of the device was tested with a maximum of five drops. A comparison of simulated and measured reflection coefficient responses is shown in Fig. 13. Fig. 14 descipted simulation measurement for five different glucose samples. Based on these plots, the theoretical and experimental setups exhibit approximately similar responses. However, the solution is complicated to position in the sensing region, which causes a sudden resonance at 8.496 GHz. In Fig. 11(b), it is shown that, regardless of the injection amount per drop (five drops), different measured responses are plotted. This indicates that the unit cell is a sensing device. The quality factor is a parameter utilized to characterize the efficacy of a resonator. In applications where a resonator is utilized as a sensing mechanism, it is imperative to monitor and assess the Q-factor in real time. Sensor performance are also measured in term of quality factor, F.D.R. and measurement error. Quality factor can be calculated by using following equation [23].

$$Q \cdot F \cdot = \frac{\lambda}{FWHM} \tag{16}$$

Where $\lambda = \frac{C}{f}$ where is c and f represent speed of light and reason frequency, and F.W.H.M. represents full width at half maximum. Frequency detection Resolution can be calculated as [28].

Table 3
Comparison with counterpart.

Ref.	Size (mm)	Materials of Substrate	Technique	Operating Frequency (GHz)	Sensitivity	Q-Factor	F.R.D. MHz	Application Method
[22]	20 × 20	RO4350B	Transmission	2–5	0.037 GHz 30 mg/dL	Nil	Nil	Non-invasive
[28]	30 × 18	RO4003	Transmission	3–10	3.5 MHz (mg/mL)	180	3.58	Non-invasive
[29]	40 × 40	Silicon	Transmission	50–67	2.2–7.7 mg/mL	Nil	Nil	Non-invasive
[30]	20 × 20	RO5880	Reflection	16.2	1.4 mg/mL	Nil	Nil	Non-invasive
[31]	52 × 24	RO5880	Reflection	8.9	150 MHz/mgmL^{-1}	50	2.56	Non-invasive
[32]	16	FR-4	Reflection	0.98	150 KHz (mg/mL)	35	0.17	Non-invasive
[33]	60 × 20	RO3210	Transmission	1.8	3.07 MHz mg/dL	Nil	Nil	non-invasive
[34]	35 × 35	RT5880	Transmission	1–8	100–500 mg/mL	Nil	Nil	Glucose Sensing
[35]	20 × 40	AI2O3	Transmission	1–6	50 mg/dL	Nil	Nil	Non-invasive
This work	6.5 × 6.5	RT5880	Reflection	8–12	0.026MHZ mg/dL	184.04	5.06	Non-invasive Glucose Sensing

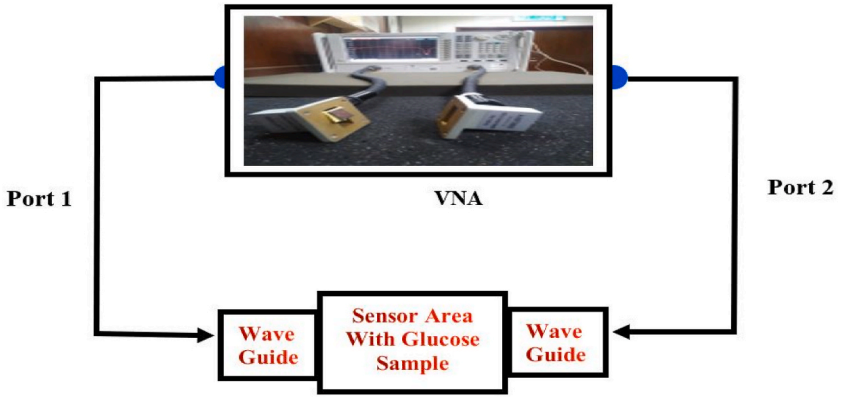

Fig. 10. Experimental Step for measurement.

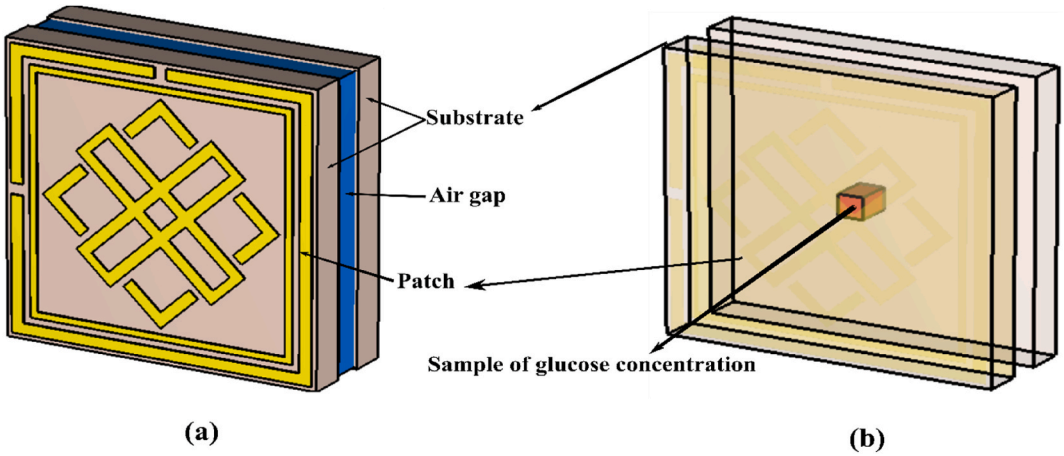

Fig. 11. (**a**) Simulation Step for glucose concentration measurement (**b**) transparent view of simulations step.

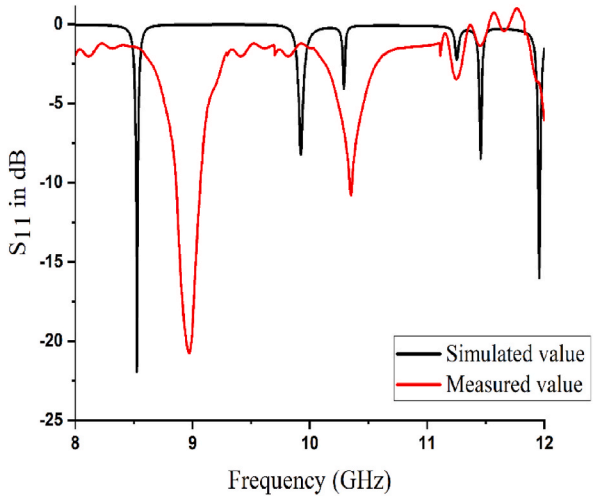

Fig. 12. Simulated vs measured reflection cofficient for glucose sample at 50 mg/dL.

$$FRD = \frac{\Delta f}{\Delta C} \tag{17}$$

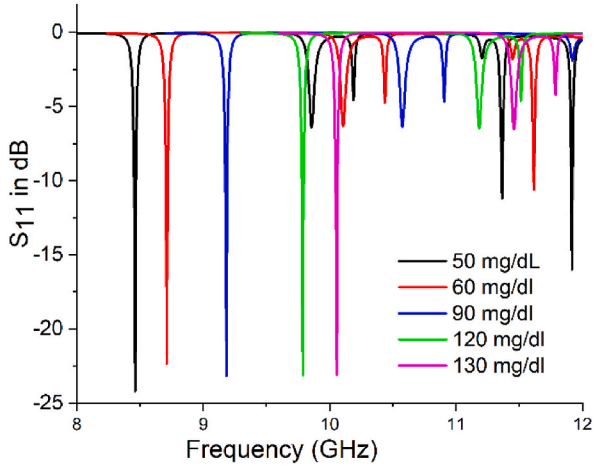

Fig. 13. Simulation reflection coefficient for different glucose samples.

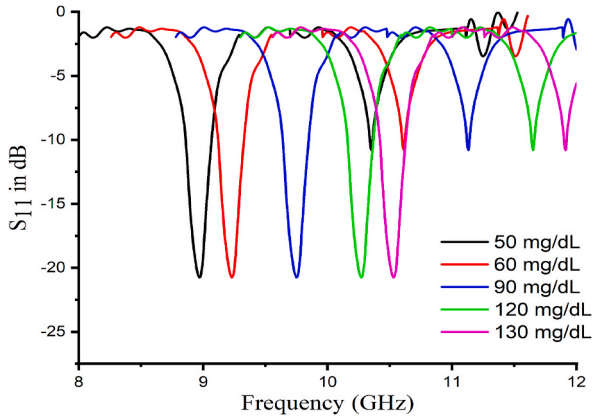

Fig. 14. Measured reflection cofficient for different glucose.

Where Δf *and*ΔC denoted the glucose variations and relatvie shift in the resonant frequency.

4. Conclusions

A novel real-time metamaterial sensor is presented in this paper based on a non-invasive method operated in microwave frequencies for the measurement of glucose levels**.** The design and analysis of this sensor were carried out using microwave simulation technology (C.S.T.) by evaluating variations in the reflection coefficient at the resonance frequency. According to simulations and measurements of glucose concentrations in water, this indicates a potential sensing capability of the sensor in the X-band, which has a double negative characteristic and maximum absorption. Additionally, changing the permittivity for concentration level from 50 mg/dL to 130 mg/dL 0.026 GHz pr step shift in resonance frequency. Further, it was found that by increasing the permittivity of the concentration level from 50 mg/dL to 130 mg/dL, there would be a shift in resonance frequency of 0.026 GHz per step. Several advantages are offered by the present metamaterial-based glucose sensor, including the ability to measure glucose levels in a sample in real-time, low cost, durability, precision, and the ability to rapidly detect glucose levels in a sample. Despite simulations, fabrication procedures have been carried out for more accurate result verification. The suggested sensor can be used for biosensing applications and human glycaemia.

Data availability statement

Data is available within the article. If someone would like to request this study's data, please contact Dr. Ahsanul Haque, corresponding author, on a reasonable request.

Funding

The author acknowledges the Fundamental Research Grants Scheme (FRGS), grant number FRGS/1/2021/TK0/MMU/01/1 funded by the Ministry of Higher Education (MOHE), Malaysia.

CRediT authorship contribution statement

Muhammad Amir Khalil: Conceptualization, Investigation, Methodology, Writing – original draft. **Wong Hin Yong:** Funding acquisition, Project administration, Supervision, Writing – original draft. **Md Shabiul Islam:** Methodology, Validation, Writing – review & editing. **Ahasanul Hoque:** Formal analysis, Supervision, Validation, Writing – original draft. **Cham Chin leei:** Writing – review & editing. **Mohamed S. Soliman:** Investigation, Validation, Writing – review & editing. **Mohammad Tariqul Islam:** Data curation, Resources, Visualization, Writing – original draft.

Declaration of competing interest

Please check the following as appropriate:

All authors have participated in (a) conception and design, or analysis and interpretation of the data; (b) drafting the article or revising it critically for important intellectual content; and (c) approval of the final version.

This manuscript has not been submitted to under review at, another journal or other publishing venue.

The authors have no affiliation with any organization with a direct or indirect financial interest in the subject matter discussed in the manuscript

The following authors have affiliations with organizations with a direct or indirect financial interest in the subject matter discussed in the manuscript.

References

[1] N.H. Cho, , et al.I.D.F. Diabetes Atlas, Global estimates of diabetes prevalence for 2017 and projections for 2045,", Diabetes Res. Clin. Pract. 138 (Apr. 2018) 271–281, https://doi.org/10.1016/j.diabres.2018.02.023.

[2] M.T. Islam, A. Hoque, A.F. Almutairi, N. Amin, Left-handed metamaterial-inspired unit cell for S-Band glucose sensing application, Sensors 19 (1) (Jan. 2019), https://doi.org/10.3390/s19010169.

[3] D. Elsheakh, Non-invasive electromagnetic biological microwave testing, in: Microwave Systems and Applications, InTech, 2017, https://doi.org/10.5772/64773.

[4] L. Lipani, et al., Non-invasive, transdermal, path-selective and specific glucose monitoring via a graphene-based platform, Nat. Nanotechnol. 13 (6) (Jun. 2018) 504–511, https://doi.org/10.1038/s41565-018-0112-4.

[5] R. Zhang, et al., Noninvasive electromagneticwave sensing of glucose, Sensors 19 (5) (2019), https://doi.org/10.3390/s19051151. MDPI AG, Mar. 01,.

[6] R. Baghbani, M.A. Rad, A. Pourziad, Microwave sensor for non-invasive glucose measurements design and implementation of a novel linear, IET Wirel. Sens. Syst. 5 (2) (Apr. 2015) 51–57, https://doi.org/10.1049/iet-wss.2013.0099.

[7] H. Choi, J. Nylon, S. Luzio, J. Beutler, A. Porch, Design of continuous non-invasive blood glucose monitoring sensor based on a microwave split ring resonator, in: Conference Proceedings - 2014 IEEE MTT-S International Microwave Workshop Series on: R.F. And Wireless Technologies for Biomedical and Healthcare Applications, IMWS-Bio 2014, Institute of Electrical and Electronics Engineers Inc., Feb. 2015, https://doi.org/10.1109/IMWS-BIO.2014.7032398.

[8] Q. Li, X. Xiao, T. Kikkawa, Noninvasive blood glucose level detection based on matrix pencil method and artificial neural Network, Journal of Electrical Engineering and Technology 16 (4) (Jul. 2021) 2183–2190, https://doi.org/10.1007/s42835-021-00719-3.

[9] W.T. Sethi, M.A. Ashraf, S.A. Alshebeili, K. Issa, Thumb positioning analysis of new elliptical-shaped microwave sensors for non-invasive glucose monitoring, Electron. Lett. 54 (9) (May 2018) 553–554, https://doi.org/10.1049/el.2018.0128.

[10] A. Ishimaru. Electromagnetic wave propagation, radiation, and scattering: from fundamentals to applications, John Wiley & Sons, 2017.

[11] A. Kandwal, et al., Highly sensitive closed loop enclosed split ring biosensor with high field confinement for aqueous and blood-glucose measurements, Sci. Rep. 10 (1) (Dec. 2020), https://doi.org/10.1038/s41598-020-60806-9.

[12] T. Yilmaz, R. Foster, Y. Hao, Towards accurate dielectric property retrieval of biological tissues for blood glucose monitoring, IEEE Trans. Microw. Theor. Tech. 62 (12) (Dec. 2014) 3193–3204, https://doi.org/10.1109/TMTT.2014.2365019.

[13] K.K. Adhikari, N.Y. Kim, Ultrahigh-sensitivity mediator-free biosensor based on a microfabricated microwave resonator for the detection of micromolar glucose concentrations, IEEE Trans. Microw. Theor. Tech. 64 (1) (Jan. 2016) 319–327, https://doi.org/10.1109/TMTT.2015.2503275.

[14] N.Y. Kim, R. Dhakal, K.K. Adhikari, E.S. Kim, C. Wang, A reusable robust radio frequency biosensor using microwave resonator by integrated passive device technology for quantitative detection of glucose level, Biosens. Bioelectron. 67 (May 2015) 687–693, https://doi.org/10.1016/j.bios.2014.10.021.

[15] S. Saha, et al., A glucose sensing system based on transmission measurements at millimetre waves using micro strip patch antennas, Sci. Rep. 7 (1) (Dec. 2017), https://doi.org/10.1038/s41598-017-06926-1.

[16] H. Cano-Garcia, et al., Reflection and transmission measurements using 60 GHz patch antennas in the presence of animal tissue for non-invasive glucose sensing, in: 2016 10th European Conference on Antennas and Propagation, EuCAP 2016, Institute of Electrical and Electronics Engineers Inc., May 2016, https://doi.org/10.1109/EuCAP.2016.7481178.

[17] S. Saha, et al., Evaluation of the sensitivity of transmission measurements at millimeter waves using patch antennas for non-invasive glucose sensing, in: 2016 10th European Conference on Antennas and Propagation, EuCAP 2016, Institute of Electrical and Electronics Engineers Inc., May 2016, https://doi.org/10.1109/EuCAP.2016.7481304.

[18] C.G. Juan, E. Bronchalo, B. Potelon, C. Quendo, E. Ávila-Navarro, J.M. Sabater-Navarro, Concentration measurement of microliter-volume water-glucose solutions using Q factor of microwave sensors, IEEE Trans. Instrum. Meas. 68 (7) (Jul. 2019) 2621–2634, https://doi.org/10.1109/TIM.2018.2866743.

[19] L. Malena, O. Fiser, P.R. Stauffer, T. Drizdal, J. Vrba, D. Vrba, Feasibility evaluation of metamaterial microwave sensors for non-invasive blood glucose monitoring, Sensors 21 (20) (Oct. 2021), https://doi.org/10.3390/s21206871.

[20] S. RoyChoudhury, V. Rawat, A.H. Jalal, S.N. Kale, S. Bhansali, Recent advances in metamaterial split-ring-resonator circuits as biosensors and therapeutic agents, in: Biosensors and Bioelectronics, vol. 86, Elsevier Ltd, 2016, pp. 595–608, https://doi.org/10.1016/j.bios.2016.07.020. Dec. 15.

[21] S. Sakib, et al., A central spiral split rectangular-shaped metamaterial absorber surrounded by polarization-insensitive ring resonator for S-band applications, Materials 16 (3) (Feb. 2023), https://doi.org/10.3390/ma16031172.

[22] M.T. Islam, A. Hoque, A.F. Almutairi, N. Amin, Left-handed metamaterial-inspired unit cell for S-Band glucose sensing application, Sensors 19 (1) (Jan. 2019), https://doi.org/10.3390/s19010169.

[23] M.A. Khalil, et al., Double-negative metamaterial square enclosed Q.S.S.R for microwave sensing application in S-band with high sensitivity and Q-factor, Sci. Rep. 13 (1) (May 2023) 7373, https://doi.org/10.1038/s41598-023-34514-z.
[24] M.A.W. Nordin, M.T. Islam, N. Misran, DESIGN OF A COMPACT ULTRAWIDEBAND META-MATERIAL ANTENNA BASED ON THE MODIFIED SPLIT-RING RESONATOR AND CAPACITIVELY LOADED STRIPS UNIT CELL, 2013.
[25] Lumped Elements for R.F. And Microwave Circuits.
[26] F.E. Terman. Radio Engineers' Handbook, The McGraw-Hill Companies, Inc, New York, NY, USA, 1943.
[27] H.E. Burton, The optics of Euclid1, in: E. Burton (Ed.), *JOSA* 35, "The Optics of Euclid'.", 1945, pp. 357–372.H.
[28] S. Kiani, P. Rezaei, M. Fakhr, Dual-frequency microwave resonant sensor to detect noninvasive glucose-level changes through the fingertip, IEEE Trans. Instrum. Meas. 70 (2021), https://doi.org/10.1109/TIM.2021.3052011.
[29] A.E. Omer, S. Gigoyan, G. Shaker, S. Safavi-Naeini, WGM-based sensing of characterized glucose- aqueous solutions at mm-waves, IEEE Access 8 (2020) 38809–38825, https://doi.org/10.1109/ACCESS.2020.2975805.
[30] H.M. Marzouk, Abd El-Hameed, A.S.A. Allam, R.K. Pokharel, A.B. Abdel-Rahman, 1-5.IEEE.H.M. Marzouk, A.S. Abd El-Hameed, A. Allam, R.K. Pokharel, A. B. Abdel-Rahman, Circular DGS Resonator for Non-Invasive Sensing of Diabetes. 2023 17th European Conference on Antennas and Propagation (EuCAP), 2023, p. 2023.
[31] A. Kandwal, et al., Surface plasmonic feature microwave sensor with highly confined fields for aqueous-glucose and blood-glucose measurements, IEEE Trans. Instrum. Meas. 70 (2021), https://doi.org/10.1109/TIM.2020.3017038.
[32] R.S. Hassan, J. Lee, S. Kim, A minimally invasive implantable sensor for continuous wireless glucose monitoring based on a passive resonator, IEEE Antenn. Wireless Propag. Lett. 19 (1) (Jan. 2020) 124–128, https://doi.org/10.1109/LAWP.2019.2955176.
[33] E. Mansour, M. I. Ahmed, A. Allam, R. K. Pokharel, and A. B. Abdel-Rahman, "A Microwave Sensor Based on Double Complementary Split-Ring Resonator Using Hexagonal Configuration for Sensing Diabetics Glucose Levels.
[34] Y.I. Abdulkarim, et al., Hypersensitized metamaterials based on a corona-shaped resonator for efficient detection of glucose, Appl. Sci. 11 (1) (Jan. 2021) 1–19, https://doi.org/10.3390/app11010103.
[35] H.A. Parsamyan, A. Zh Babajanyan, S. Kh Arakelyan, K. Lee, A. Zh Babajanyan, S. Kh Arakelyan, Math-Net.Ru ?бщероссийский МатеМатический портал determination of glucose concentration in aqueous solution by using modified hilbert shaped microwave metamaterial sensor [Online]. Available: http://www.mathnet.ru/rus/agreement, 2018.
[36] K.K. Sethi, G. Palai, P. Sarkar, Realization of accurate blood glucose sensor using photonics based metamaterial, Optik 168 (Sep. 2018) 296–301, https://doi.org/10.1016/j.ijleo.2018.04.091.